Am J Transl Res 2025;17(8):6573-6586
www.ajtr.org /ISSN:1943-8141/AJTR0164335

Original Article

Chemotherapy-induced suppression of colorectal cancer-associated gut microbiota and modulation of host miRNA expression

Chunli Wang[1*], Baoyang Kuang[2,3*], Kuan Yang[2,3], Xuewen Xiao[4], Caixia Wu[2,3], An Li[2,3], Xiaoli Zeng[2,3], Xiangcai Wang[2,3], Jianming Ye[2,3]

[1]*Intensive Care Unit, First Affiliated Hospital, Gannan Medical University, Ganzhou 341000, Jiangxi, China;* [2]*Department of Oncology, First Affiliated Hospital, Gannan Medical University, Ganzhou 341000, Jiangxi, China;* [3]*Jiangxi Clinical Medical Research Center for Cancer, Ganzhou 341000, Jiangxi, China;* [4]*Department of Pathology, First Affiliated Hospital, Gannan Medical University, Ganzhou 341000, Jiangxi, China.* [*]*Equal contributors.*

Received March 5, 2025; Accepted July 18, 2025; Epub August 15, 2025; Published August 30, 2025

Abstract: Objectives: To characterize gut microbiome alterations in colorectal cancer (CRC) patients following cancer chemotherapy (CCT) and to explore associations with bacterial translocation and host miRNA dynamics. Methods: Stool samples were prospectively collected from 20 CRC patients who had undergone radical surgery followed by adjuvant chemotherapy (CAPOX/mFOLFOX6). Stool samples were collected pre- and post-CCT. Microbial profiling was performed using 16S rRNA sequencing. Bacterial translocation was assessed by measuring serum anti-Lipopolysaccharides (LPS) IgA/IgG levels by ELISA. miRNA expression of miR-143 and miR-145 was quantified using qPCR. Results: Post-CCT samples showed significant increases in gut microbiome diversity ($P<0.05$), with higher relative abundances of *Porphyromonas*, *Peptostreptococcus*, and *Parvimonas,* and decreased abundances of *Faecalibacterium* and *Ruminococcaceae* ($P<0.005$). Network analysis identified *Peptostreptococcus* and *Parvimonas* as possible CRC-associated taxa. Serum anti-LPS IgA and IgG levels significantly declined post-CCT, indicating reduced bacterial translocation. Concurrently, miR-143 and miR-145 levels increased more than twofold post-CCT ($P<0.01$), positively correlating with microbial shifts. Conclusion: CCT induces significant remodeling of CRC-associated gut microbiota, characterized by suppression of pathogenic genera and enrichment of pro-inflammatory taxa. These changes align with reduced bacterial translocation and increased expression of tumor-suppressive miRNAs, suggesting that CCT exerts dual therapeutic effects by simultaneously modulating microbial communities and host molecular pathways.

Keywords: Gut microbiome, colorectal cancer, chemotherapy, 16S rRNA, bacterial translocation, miRNA

Introduction

Colorectal cancer (CRC) pathogenesis involves complex interactions between genetic predisposition and environmental factors [1]. Among environmental influences, lifestyle and dietary habits have been clinically confirmed as major contributors to CRC risk. Emerging evidence suggests that dietary patterns can significantly modulate the gut microbiome, thereby contributing to the pathogenesis of CRC [2-8].

Advances in next-generation sequencing and related technologies have enabled detailed investigations into the role of the microbiome in CRC pathogenesis [9-13]. Studies have shown that the diversity and composition of gut microbiome in CRC patients are altered compared to healthy individuals. Characteristic strains in CRC patients mainly included *Clostridium*, *Bacteroides*, *Streptococcus digest*, and *Pseudomonas parvum*. Comparative analyses of fecal samples from CRC patients and individuals with normal colonoscopy findings have consistently reported elevated levels of *Bacteroides* and *Prevotella* in CRC patients. Additionally, specific bacteria such as *Clostridium nucleatum*, *Akkermansia muciniphila*, *Eubacterium hallii*, *Eubacterium eligens*, and *Eubacterium rectale*, have been implicated in CRC develop-

https://doi.org/10.62347/XXCS3377

ment [14]. A lipid-dependent basidiomycete yeast of normal skin microbiota, *Malassezia*, has also been detected in the intestinal microbiota of CRC patients [15]. The gut microbiome is increasingly recognized as a promising source of non-invasive biomarkers for early CRC detection [16-18].

Although the mechanistic links between gut microbiota and CRC remain incompletely characterized, Gram-negative bacterial enrichment in CRC patients may promote carcinogenesis through Lipopolysaccharide (LPS)-induced inflammation [19-21]. LPS present on the outer membranes of these bacteria can trigger an inflammatory signal cascade through Toll-like receptor 4 (TLR4) on epithelial cells. Furthermore, the gut microbiota modulate mucosal immune response, with significantly increased infiltration of IL-17-producing immune cells observed in the colonic mucosa of CRC patients. Studies have also shown that *Candida albicans* affects the occurrence and development of CRC through its immunomodulatory effects [22]. In a clinical trial evaluating Regorafenib combined with Toripalimab for metastatic CRC, non-responders exhibited a significantly higher relative abundance and positive detection rate of *Clostridium* [23].

Recent evidence suggests that intestinal microbiota may influence both the efficacy and toxicity of cancer chemotherapy (CCT) in CRC patients [24, 25]. Regulating the intestinal microbiome before and during CCT can enhance therapeutic efficacy and reduce treatment-related adverse events. However, comprehensive statistical data on microbiome changes before and after CCT remain limited. To address this gap, this study analyzed the gut microbiota composition in CRC patients before and after CCT to assess the effect of CCT on microbial structure. Additionally, as certain miRNAs have been reported as potential molecular markers for CRC [26], we investigated how their levels correspond to gut microbiota alterations following CCT.

Materials and methods

Study design

This prospective observational cohort study was conducted at the First Affiliated Hospital of Gannan Medical University between July 2020 and June 2021. All patients had completed radical surgery and adjuvant chemotherapy (CAPOX or mFOLFOX6) prior to enrollment. No study-specific interventions were administered; all treatments were part of routine clinical care. The research protocol involved prospective collection of stool samples and clinical data only.

A total of 20 patients who completed treatment were prospectively enrolled. Inclusion criteria: (1) Adults (45-70 years) with pathologically confirmed CRC; (2) Completion of radical surgery followed by standardized chemotherapy; (3) No exposure to antibiotics within 3 months before enrollment. Exclusion criteria: (1) Evidence of metastatic CRC, inflammatory bowel disease, or other malignancies; (2) Use of probiotics or immunosuppressive agents during the study period; (3) Prior chemotherapy before the current treatment course.

Antibiotic exposure was limited to routine perioperative prophylaxis with ornidazole (0.5 g) and cephalosporin (2 g), administered twice daily for 3 days pre- and post-surgery, as per institutional protocols.

Sample collection

Stool samples were collected at: (1) 3 weeks post-surgery (pre-CCT, Group A), and (2) 3 weeks post-chemotherapy (post-CCT, Group B).

Chemotherapy regimens

All patients received either CAPOX (capecitabine + oxaliplatin) or mFOLFOX6 regimens (leucovorin + 5-fluorouracil + oxaliplatin) post-surgery.

Outcome measurements

Primary Outcomes: Gut microbiome diversity (Shannon/Chao1 indices), differential microbial taxa (identified by LEfSe analysis), and bacterial translocation biomarkers (serum anti-LPS IgA/IgG via ELISA). Secondary Outcomes: expression of tumor-suppressive miRNAs (miR-143, miR-145) quantified by qPCR, demographic and clinical variables (age, sex, chemotherapy regimen), and microbial taxa abundance at genus and species levels.

16S rRNA analysis of microbial DNA and bioinformatics

The gut microbiome composition before and after CCT in 20 CRC patients was analyzed

using 16S rRNA gene sequencing. Sequencing was performed by BIOTREE Co., Ltd. on the Illumina HiSeq 2500 platform. To ensure high-quality and reliable data, comprehensive bioinformatic analyses were conducted, comprising the following steps: Quality Filtering: Raw reads were filtered to remove low-quality sequences, retaining those with a Phred score ≥20 over at 90% of the bases. Double-Ended Sequence Splicing: Paired-end reads were merged based on overlapping regions, requiring a minimum overlap length of 10 base pairs. Chimera Removal: Chimeric sequences were identified and removed using the UCHIME algorithm to reduce false-positive results.

Enzyme-linked immunosorbent assay (ELISA)

Serum levels of IgA, IgG and IgM antibodies against LPS and flagellin were determined using commercial ELISA kits (Invitrogen) [24]. In short, serum samples were diluted 1:200 and added to antigen-coated wells. After incubation and washing, wells were incubated with horseradish peroxidase (HRP)-conjugated secondary antibodies specific for human IgA, IgG, or IgM. All samples were measured in triplicate, and case samples were assayed on the same plate to minimize inter-assay variability.

Reverse transcription and qPCR

Total RNA was extracted from tissue samples using TRIzol reagent (Invitrogen) following the manufacturer's protocol. RNA purity and concentration were assessed using spectrophotometry (NanoDrop). cDNA was synthesized using a miRNA-specific reverse transcription kit (e.g., TaqMan MiRNA Reverse Transcription Kit, Thermo Fisher). qPCR was performed using SYBR Green Master Mix (Applied Biosystems) on a QuantStudio 5 Real-Time PCR System. Thermal cycling conditions: 95°C for 2 min (initial denaturation), 45 cycles of 94°C (15 s), 55°C (15 s), and 68°C (30 s). miRNA expression levels were quantified using the 2^(-ΔΔCt) method. Primers are listed in Supplementary Table 1.

Statistical analysis

Microbiome data were analyzed using QIIME2 (v2021.11), while clinical and biomarker data were processed with R (v4.1.2). Alpha diversity metrics (Shannon, Chao1) between pre- and post-CCT samples were compared using paired Wilcoxon signed-rank tests. Beta diversity (Bray-Curtis dissimilarity) was evaluated by permutational multivariate analysis of variance (PERM ANOVA) with 999 permutations. Pairwise comparisons between pre- and post-CCT groups were performed using Student's t-tests or Mann-Whitney U tests, depending on data distribution assessed by Shapiro-Wilk test. Correlations between microbial taxa and miRNA levels were evaluated using Spearman's rank correlation coefficient. Multiple testing correction was applied using the Benjamini-Hochberg method where appropriate. Data were presented as mean ± SEM, unless otherwise specified. Differentially abundant taxa were determined using DESeq2 (negative binomial Wald test), with statistical significance thresholds set at a false discovery rate (FDR)-adjusted $P<0.05$. For clinical biomarker associations (e.g., IgA/IgG/IgM levels), odds ratios (ORs) and 95% confidence intervals (CIs) were calculated using logistic regression. A two-tailed p-value <0.05 was considered significant.

Results

General characteristics of the gut microbiome in CRC patients

Stool samples were prospectively collected from 20 CRC patients. To assess the adequacy of sequencing depth, rarefaction curve analysis was first performed. The curves for both pre- and post-CCT samples plateaued, indicating that sequencing depth was sufficient for downstream microbial abundance analysis (**Figure 1A**). Then, species accumulation curves at the genus level were used to evaluate the richness of annotated species. The results showed that the number of shared taxa approached saturation, further confirming that sample size was sufficient for subsequent analyses (**Figure 1B**).

Differences in the gut microbiome before and after chemotherapy

A significant increase in alpha diversity was observed following CCT (**Figure 1C**). Principal component analysis (PCA) revealed a clear separation between pre- and post-CCT samples,

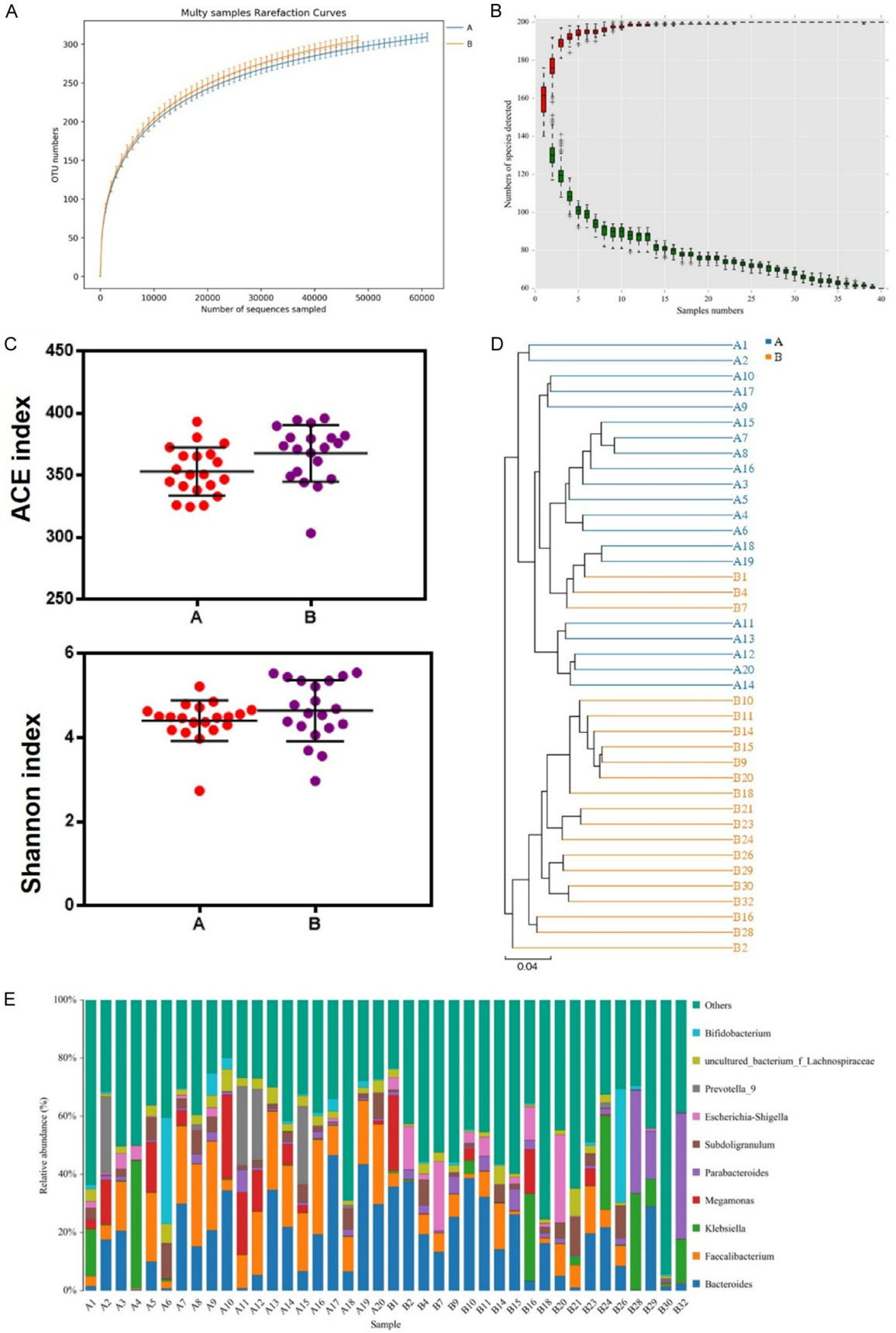
A
Multy samples Rarefaction Curves
OTU numbers
Number of sequences sampled
A
B
B
Numbers of species detected
Samples numbers
C
ACE index
Shannon index
A
B
D
A
B
0.04
E
Relative abundance (%)
Sample
Others
Bifidobacterium
uncultured_bacterium_f_Lachnospiraceae
Prevotella_9
Escherichia-Shigella
Subdoligranulum
Parabacteroides
Megamonas
Klebsiella
Faecalibacterium
Bacteroides

Figure 1. Characteristics of gut microbiome composition in CRC patients pre-CCT and post-CCT. A. Dilution curve. Each curve represents a sample and is marked with different colors. Blue and Yellow are post-CCT, Group A; and pre-CCT, Group B. (2) 3 weeks post-chemotherapy (post-CCT, Group B). B. Species accumulation curve. The x-axis represents the sample size; The y-axis represents the number of species after sampling; Red box boxplot represents the species accumulation curve; The green boxplot illustrates the curve of shared (common) species across samples. C. Alpha diversity index analysis. D. Principal component analysis (PCA). E. Genus-level taxonomic composition.

Table 1. Differential abundant genera between before- and after- CCT in gut microbiome of CRC patients according to rank sum test

Genus	A (Mean)	B (Mean)	Fold change	p
Porphyromonas	7.75E-05	0.017506	225.9901	0.000966
Peptostreptococcus	6.46E-05	0.002443	37.81211	0.000966
Parvimonas	0.00018	0.004493	24.89841	1.18E-05
Prevotellaceae_UCG-003	5.19E-06	0.000109	20.98434	1.81E-05
Eisenbergiella	9.35E-05	0.001647	17.60731	0.001702
Gemella	0.000117	0.001992	17.06955	0.002561
[Clostridium]_innocuum_group	9.65E-05	0.001542	15.98744	0.000622
Catabacter	1.80E-05	0.000183	10.19235	0.000592
Rikenellaceae_RC9_gut_group	7.18E-05	0.000386	5.373743	8.77E-05
Fusicatenibacter	0.00223	0.001466	0.657373	0.000152
Lachnospiraceae_ND3007_group	0.000561	0.00022	0.391291	0.001064
Agathobacter	0.038875	0.014024	0.360757	0.002449
Ruminococcaceae_UCG-013	0.003568	0.001277	0.357819	0.002449
Faecalibacterium	0.173445	0.052061	0.300156	0.000234
[Eubacterium]_ventriosum_group	0.004724	0.000847	0.179255	0.000437

suggesting distinct shifts in microbial community structure (**Figure 1D**). Pre-CCT samples exhibited higher inter-individual variability (**Table 1**). Differentially abundant genera between groups included *Bifidobacterium, lachnospiraceae, Prevotella_9, Escherichia-Shigella, Subdoligranulum, Parabacteroides, Megamonas, Klebsiella, Faecalibacterium* and *Bacteroides* (**Figure 1E**).

To further explore microbial structure, representative sequences were used for taxonomic annotation and comparative analysis (**Figure 2**). At the genus level, hierarchical clustering based on abundance similarity showed that pre- and post-CCT samples clustered into two distinct branches (**Figure 3**). Within-group similarity was evident, while significant compositional differences were observed between the groups.

Differential genus-level changes in the gut microbiome before and after chemotherapy

At the genus level, ANOVA was employed to assess differences in microbial abundance between pre- and post-CCT samples. The results showed that *Prevotellaneae_Ugg-003* was significantly enriched following CCT, whereas *Prevotella_9* and *Faecalibacterium* were significantly reduced (**Figure 4A**). Furthermore, the rank-sum test identified 15 genera with significant abundance changes post-CCT, including 7 genera that increased and 8 genera decreased (**Figure 4B**).

To further characterize taxa associated with treatment, linear discriminant analysis effect size (LEfSe) was performed. The resulting LDA histogram indicated that 17 bacterial taxa were significantly enriched in pre-CCT samples, while 10 taxa were enriched in post-CCT samples (**Figure 5**), suggesting a marked shift in microbial composition in response to chemotherapy.

Network analysis of gut microbiome interactions

To investigate microbial co-occurrence patterns, correlation network analysis was conducted based on genus-level abundance data

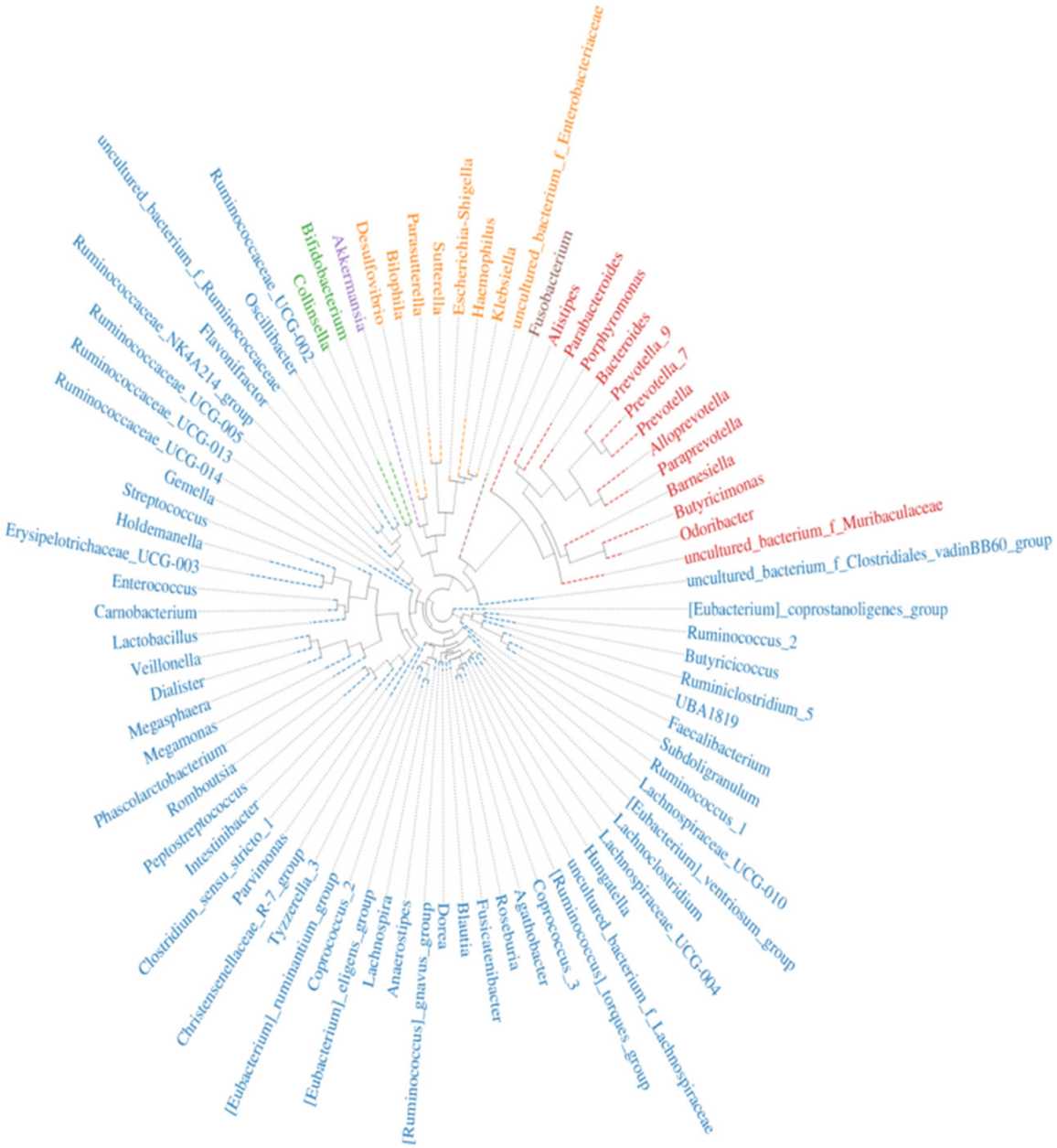

Figure 2. Phylogenetic tree of the gut microbiome at the genus level before and after CCT. Genera belonging to the same phylum are indicated by the same color.

(**Figure 6**). Within this network, several key nodes with strong intra-network correlations were identified. For instance, *Alistipes* and *Ruminococcaceae_UCG-002* exhibited the strongest positive correlation, followed by *Parvimonas* and *Peptostreptococcus*. Additionally, *Ruminococcaceae_NK4A214*_group showed a strong negative correlation with *Clostridium_innocuum_group*.

Bacterial translocation was reduced following CCT

We measured serum biomarkers in CRC patients before and after chemotherapy to validate bacterial translocation. The associations between these biomarkers and CCT are detailed in **Table 2**. Among the evaluated indicators, anti-flagellin IgA was significantly asso-

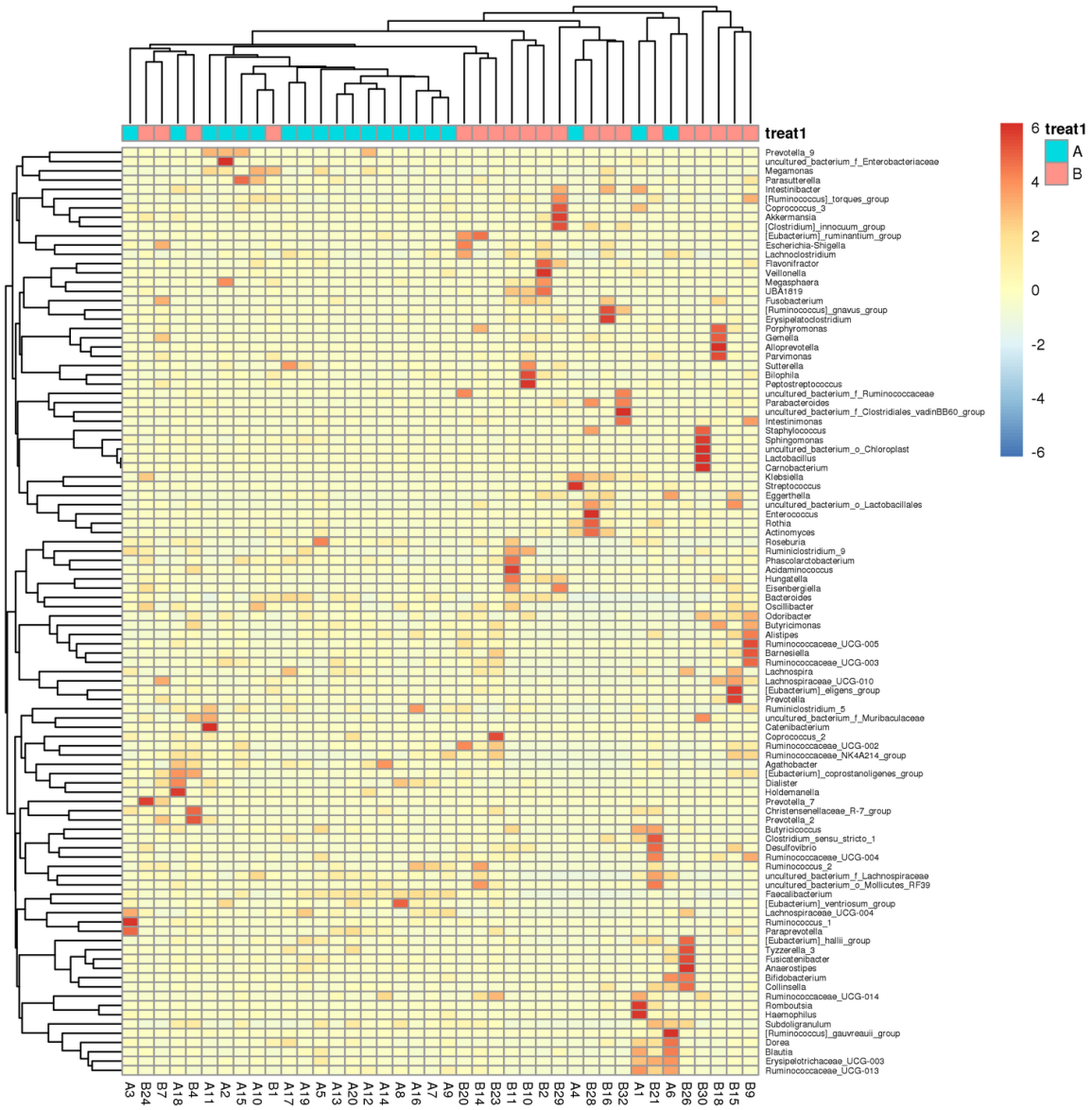

Figure 3. Heatmap of species abundance clustering at the genus level before and after chemotherapy. The heatmap displays hierarchical clustering of gut microbiota based on standardized relative abundance (Z-scores) of each genus.

ciated with post-CCT status (OR=4.5, P=0.025). Furthermore, anti-LPS IgA showed the strongest inverse association with post-CCT status (OR=5.57, P=0.011), consistent with reduced translocation (**Table 2**). Similarly, anti-LPS IgG showed an association with CCT (OR=4.5, $P<0.05$). Collectively, these results suggest that systemic exposure to bacterial components is significantly reduced after chemotherapy, as evidenced by decreased levels of translocation-related antibodies.

Host miRNA changes in CRC patients after chemotherapy

Several circulating miRNAs (miRNAs) have been identified as potential molecular markers for CRC. For instance, miR-21, miR-31 and miR-106a levels are elevated in peripheral blood of CRC patients compared to healthy individuals, while the levels of miR-135a, miR-135b, miR-143 and miR-145 are typically downregulated [32, 33].

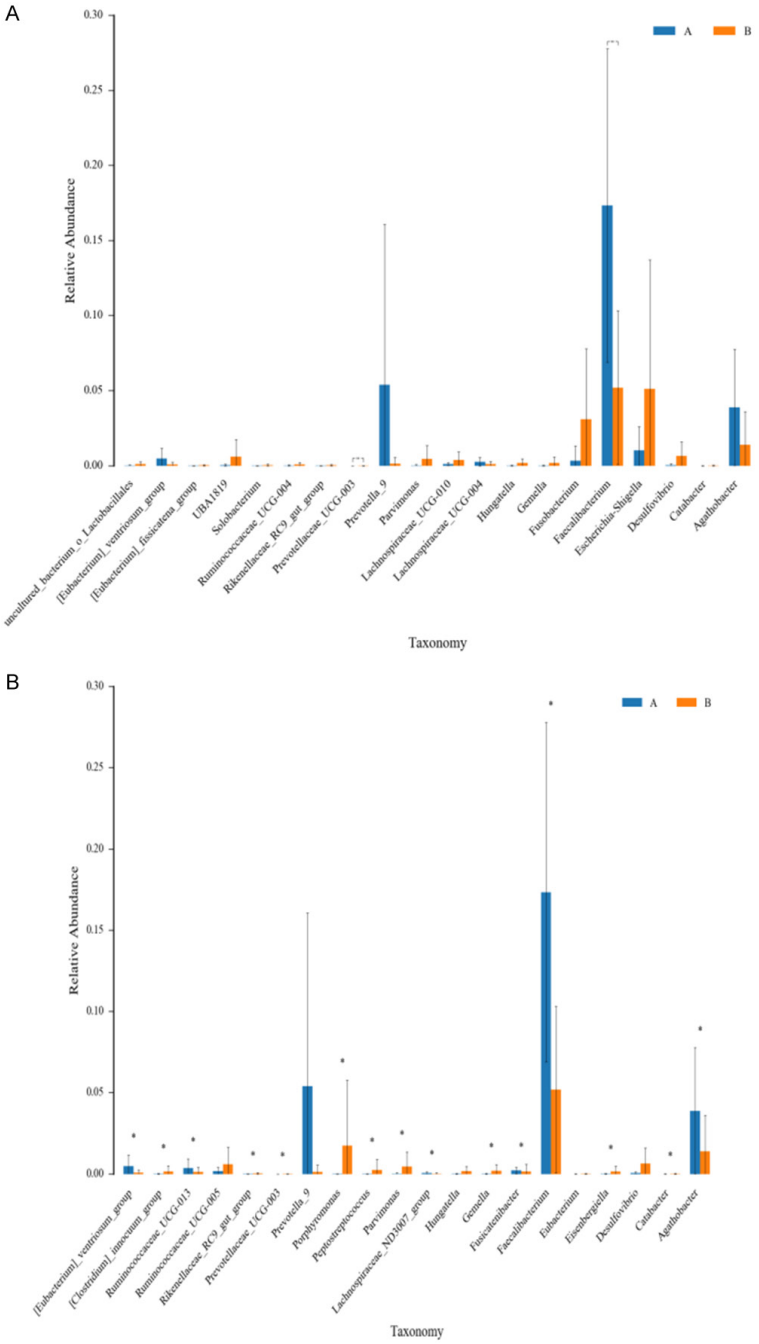

Figure 4. Differential species analysis of the gut microbiome before and after CCT in CRC patients. A. ANOVA analysis. B. Rank sum test. * indicates P<0.05.

Using quantitative PCR, we measured the expression of these miRNAs in patients before (Group A) and after chemotherapy (Group B). The results showed that miR-21, miR-31 and miR-106a levels were significantly reduced in group B compared to Group A. In contrast, mir-R35a, miR-135b, miR-143 and miR-145 levels were significantly increased after CCT (**Figure 7**). While most miRNAs showed statistically significant differences, only miR-143 and miR-145 demonstrated more than a twofold increase post-CCT.

Discussion

Intestinal microbiota are closely linked not only to disease pathogenesis but also to treatment response and therapeutic efficacy in a range of clinical conditions [27-31]. Using high throughput 16S rRNA amplicon sequencing, we identified significant changes in gut microbiota of CRC patients before and after CCT.

Notably, microbial diversity increased post-CCT, with significant enrichment in several genera, including *Porphyromonas, Peptostreptococcus, Parvimonas, Prevotellaceae_*UCG-003*, Eisenbergiella, Gemella, [Clostridium]_innocuum_group, Catabacter, and Rikenellaceae_RC9_gut_group*. Some of them were reported related to the development and progress of CRC. For instance, *Porphyromonas gingivalis,* a well-known periodontal pathogen, has been been reported to promote CRC development through inflammatory pathways [23]. Other enriched genera, though not directly linked to CRC in current literature, have been confirmed to correlate with *porphyrinomonas* in other inflammatory diseases. For example, a negative correlation has been observed between *Porphyromonas* and *Streptococcus* abundance, with *Porphyromonas* increasing and *Streptococcus* decreasing in certain disease contexts [32]. In the oral microbiome, *Gemella haemolysans* has been shown to suppress *P. gingivalis* growth, suggesting complex microbial antagonism [33]. In Radical Colorectal Surgery (RCS), genera such as

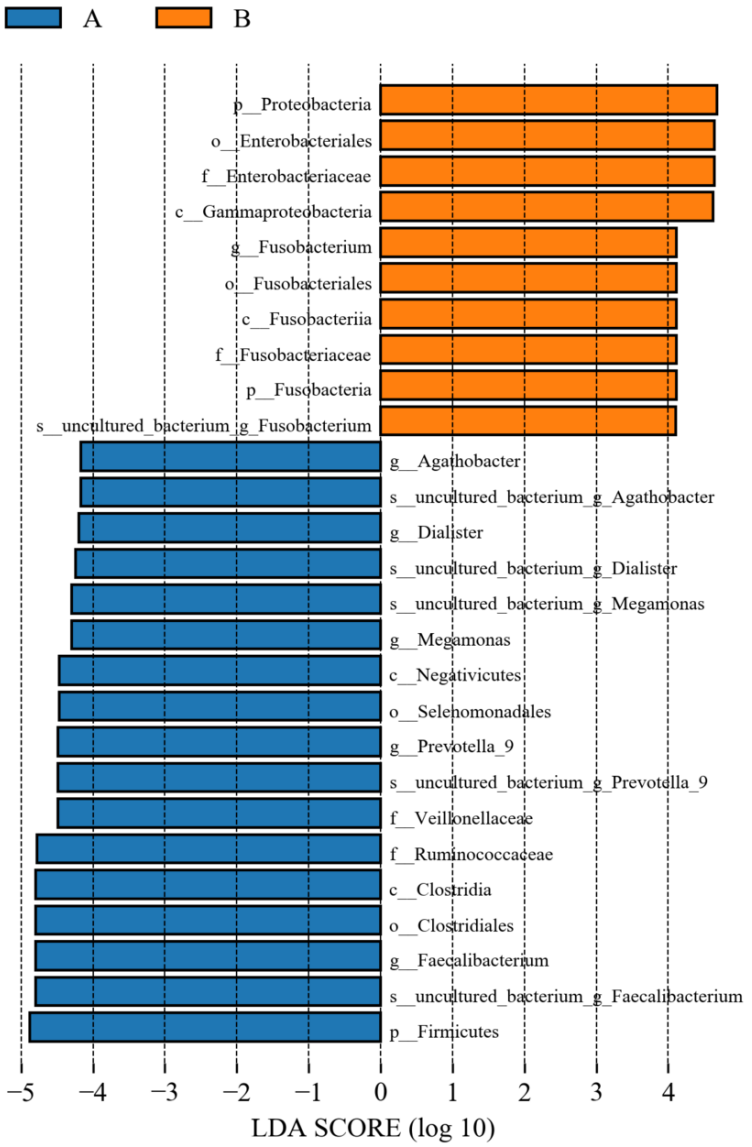

Figure 5. Line discriminant analysis (LEfSe) of gut microbiome differences before and after CCT in CRC patients.

Enterococcus, *Vibrio parvus* and *Stomatal bacilli* are predominant, while in palliative surgery (PPS), the dominant bacteria include *Enterococcus*, *Vibrio parvus*, *stomata*, *digestive Streptococcus* and *Clostridium* [34]. These findings demonstrate that CCT can drive heterogeneous but meaningful remodeling of CRC-associated gut microbiota, characterized by the depletion of beneficial taxa such as Faecalibacterium, and the enrichment of potentially pro-inflammatory or opportunistic genera.

Following CCT, a marked decrease was observed in the abundance of several gut microbial taxa, including *Fusicatenibacterr, Lachnospiraceae_ND3007_group, Agathobacter, Ruminococcaceae_UCG-013, Faecalibacterium, and [Eubacterium]_ventriosum_*group. Previous studies have reported that in the gut microbiota of CRC patients, the abundance of potentially pathogenic or pro-inflammatory taxa such as *Clostridium, Candida, Porphyromonadaceae, Coriobacteriaceae, Staphylococcaceae, Akkermansia*, and *Methanobrevibacter* is elevated. In contrast, beneficial genera such as *Bifidobacterium, Lactobacillus, Ruminococcus, Faecalibacterium, Roseburia*, and *Treponema* are consistently reduced. Although several of the species showing decreased abundance post-CCT in our study have not been directly linked to CRC, they are known to interact with core commensals like *Faecalibacterium* and *Ruminococcus*. For example, in infant feces, the abundances of *Bacteroides, Unclassified chlamydia, Fecal bacilli, Ackermann* and *Phascolarctobacter* were negatively correlated with the abundances of *Escherichia coli, Bifidobacteria, Intravenous pull bacteria* and *Streptococcus* [35]. In the ileum and cecum, *Faecalibacterium* abundance has also been associated with variations in the abundance of other bacilli [36]. The marked depletion of beneficial genera like *Faecalibacterium* and *Ruminococcaceae* underscores the dual nature of CCT - while effective against CRC, it may inadvertently disrupt protective microbial niches.

A recent study evaluating FOLFIRI scheme reported differential bacteria taxa, including reductions in *Fecobacteria, Clostridium, Phascolactobacterium, Humicola, and Rhodotorula, and increases in Candida, Magnetobacteria, tremella, Bacillus bimodus,* and *Saccharomycetes* [37]. Notably, the decrease in

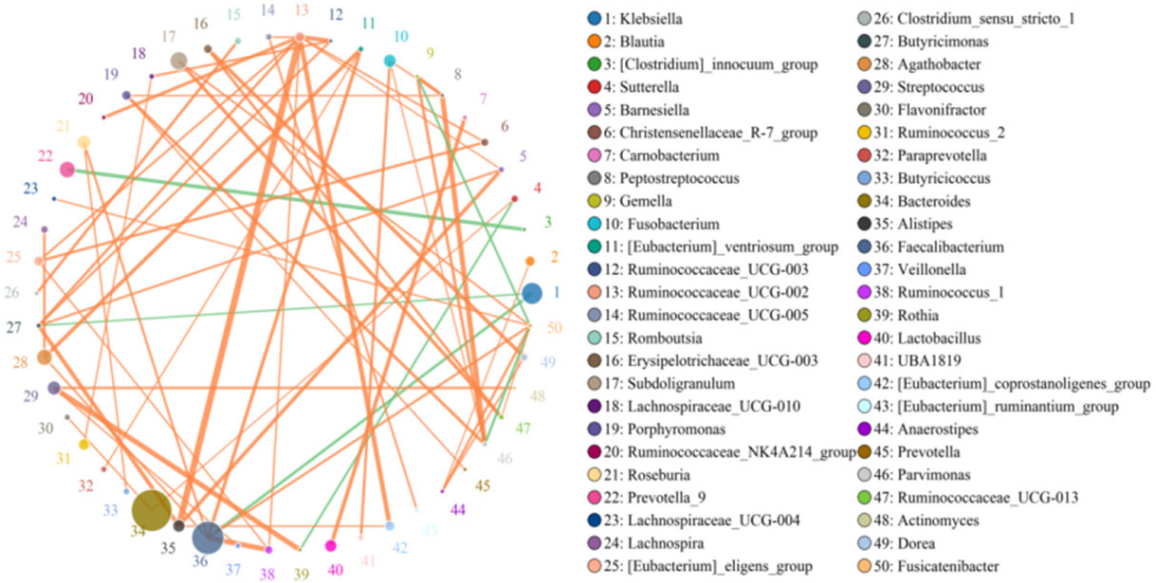

Figure 6. Network analysis of differential species.

Table 2. Associations between biomarkers of bacterial translocation and CCT in CRC patients

	b-CCT	a-CCT	OR	95% CI		X^2	p-CHI
anti-flagellin IgA	9	6	4.50	1.166	5.414	5.01	0.025
anti-flagellin IgG	6	5	1.29	0.319	2.533	0.13	0.723
anti-flagellin IgM	6	6	1.00	0.259	2.436	0	1
anti-LPS IgA	11	5	5.57	1.420	6.391	6.46	0.011
anti-LPS IgG	9	5	4.50	1.166	5.414	5.01	0.025
anti-LPS IgM	6	5	1.29	0.319	2.533	0.13	0.723

Anti-flagellin IgA showed a significant association with CCT (OR=4.5, P=0.025). Anti-LPS IgA exhibited the strongest association (OR=5.57, P=0.011). Anti-LPS IgG also demonstrated an association (OR=4.5). These results suggest a significant reduction in bacterial translocation in patients following CCT.

Faecalibacterium observed in that study aligns with our findings. Another study analyzing gut microbiota in patients with stage II-IV CRC undergoing various chemotherapy regimens identified changes in *Bacteroides, Firmicutes, Bifidobacterium, Collinsella, Butyromonas, Eggerthella, Morganella, Trypanosoma-like taxa, Proteus, Escherichia coli, and Shigella* [14]. However, the microbial changes reported were largely inconsistent with both our study and the previous FOLFIRI-based findings, highlighting the considerable heterogeneity in chemotherapy-induced gut microbiota alterations across studies.

Our network analysis further revealed strong correlations among key taxa in post-CCT microbial communities, such as *Alistipes* with *Ruminocaceae, Parvimonas* with *Peptostreptococcus.* A notable negative correlation was observed between *Ruminocaceae* and the *Clostridium_innocuum_group*. Among these, *Peptostreptococcus* has been identified in multiple studies as a CRC-associated taxon, with elevated abundance serving as a potential predictive marker for CRC development. Likewise, increasing evidence links *Alistipes* and *Parvimonas* with CRC pathogenesis [38]. It was found that through network analysis, most of the bacteria with strong correlation with the changes of gut microbiome after CCT are the marker species of CRC [5, 39, 40]. Our network analysis identified *Peptostreptococcus* and *Parvimonas* as central nodes in post-CCT microbial communities, reinforcing their potential role as therapeutic targets or prognostic biomarkers in CRC management.

This study investigated alterations in intestinal flora and miRNA expression before and after radical CRC surgery, particularly after the first chemotherapy session. To reduce confounding effects, stool samples were collected three weeks post-surgery, allowing time for the imme-

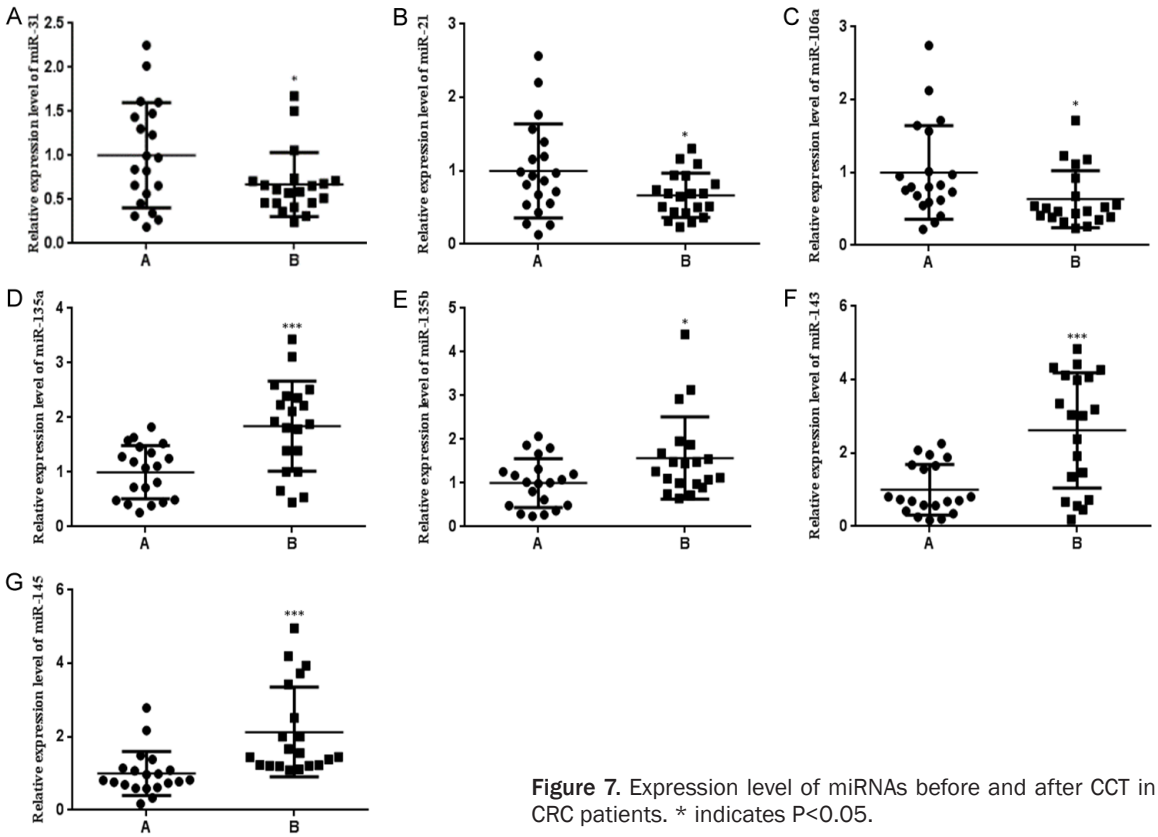

Figure 7. Expression level of miRNAs before and after CCT in CRC patients. * indicates P<0.05.

diate physiologic and inflammatory responses to stabilize. Both antibiotic use and surgery were recognized as potential confounders. Surgical intervention can disrupt intestinal homeostasis through inflammatory and mechanical pathways, while antibiotics can alter gut microbial composition. In this study, perioperative antibiotic use was documented and analyzed.

It has been reported that the expression of host miRNA is related to the gut microbiome. For instance, during *Listeria monocytogenes* infection, the expression of six miRNAs-miR-143, miR-148a, miR-200b, miR-200c, and miR-378 - was significantly reduced in conventionally raised mice [26]. Notably, these changes were shown to be microbiota-dependent, underscoring the regulatory influence of gut microbes on host gene expression. Similarly, in patients with liver cirrhosis, alterations in gut microbial composition were accompanied by significant changes in hepatic and circulating levels of miR-122 and miR-145 [38]. In another study exploring the P70S6K1/HIF1 α axis in colitis models and LPS - stimulated CCD-18co colonic myofibroblasts, miR-145 expression was found to be altered in association with gut microbiota dysbiosis [26]. Likewise, changes in miR-143 expression were reported to be influenced by microbiota status in the context of oral Listeria infection, further supporting a microbiota-miRNA interaction network [26, 31].

Our study showed a significant post-chemotherapy increase in miR-143 and miR-145-two well-recognized tumor-suppressive miRNAs in colorectal cancer - alongside marked restructuring of the gut microbiome. The concordant elevation of these miRNAs with chemotherapy-induced microbial shifts suggests a synergistic crosstalk between microbial remodeling and host molecular regulation. This interaction may contribute to enhanced therapeutic responses and deserves further mechanistic investigation in CRC.

Limitations of the study

This study has several limitations. First, the small sample size (n=20) and absence of a healthy control group limit the statistical power

and generalizability of the findings. Second, while perioperative antibiotics (ornidazole and cephalosporins) were consistently administered, their specific effects on gut microbiota were not independently analyzed, potentially confounding the observed microbial shifts. Third, sampling interval, 3 weeks post-surgery and post-chemotherapy, may not fully eliminate residual effects of surgical stress or antibiotics. Finally, the direct regulatory mechanisms linking microbiota influence of surgical stress or antibiotic exposure, potentially affecting baseline stability. Moreover, the mechanistic relationship between microbiota alterations and host miRNA expression (e.g., miR-143/miR-145) remain unelucidated. No functional or metabolomic analyses were performed to validate microbial activity, limiting the depth of biological interpretation. These factors collectively constrain causal inference and clinical translatability.

Conclusion

Our study provides significant insight into the effects of surgery and chemotherapy on the gut microbiome and host molecular regulation in colorectal cancer (CRC) patients. The results demonstrate a significant reduction in CRC-associated pathogenic bacteria genera following treatment, suggesting that microbiota remodeling mediates therapeutic benefits by suppressing pathogenic genera. Additionally, although the observed changes in tumor-suppressive miRNAs (miR-143 and miR-145) were not directly correlated with the microbiota in this study, the co-occurrence of these changes supports the hypothesis of microbiota-host molecular crosstalk during CRC treatment. These findings underscore the importance of integrating microbial and molecular factors in the comprehensive management of CRC.

Acknowledgements

The work was supported by the Science and Technology Plan Project Funded by Jiangxi Province Health Commission (grant no. 202410340).

Written informed consent was obtained from all participants prior to sample collection.

Disclosure of conflict of interest

None.

Address correspondence to: Jianming Ye and Xiangcai Wang, Department of Oncology, First Affiliated Hospital, Gannan Medical University, Ganzhou 341000, Jiangxi, China. E-mail: yejianming@gmu.edu.cn (JMY); wangxiangcai@csco.ac.cn (XCW)

References

[1] De Silva S, Tennekoon KH and Karunanayake EH. Interaction of gut microbiome and host microRNAs with the occurrence of colorectal and breast cancer and their impact on patient immunity. Onco Targets Ther 2021; 14: 5115-5129.

[2] Zhang Y, Zhu M, Dai Y, Gao L and Cheng L. Research progress in ulcerative colitis: the role of traditional chinese medicine on gut microbiota and signaling pathways. Am J Chin Med 2024; 52: 2277-2336.

[3] Xu H, Wang Y, Liu G, Zhu Z, Shahbazi MA, Reis RL, Kundu SC, Shi X, Zu M and Xiao B. Nano-armed limosilactobacillus reuteri for enhanced photo-immunotherapy and microbiota tryptophan metabolism against colorectal cancer. Adv Sci (Weinh) 2025; 12: e2410011.

[4] Liang L, Kong C, Li J, Liu G, Wei J, Wang G, Wang Q, Yang Y, Shi D, Li X and Ma Y. Distinct microbes, metabolites, and the host genome define the multi-omics profiles in right-sided and left-sided colon cancer. Microbiome 2024; 12: 274.

[5] Bhatnagar K, Jha K, Dalal N, Patki N, Gupta G, Kumar A, Kumar A and Chaudhary S. Exploring micronutrients and microbiome synergy: pioneering new paths in cancer therapy. Front Immunol 2024; 15: 1442788.

[6] Feizi H, Rezaee MA, Ghotaslou R, Sadrkabir M, Jadidi-Niaragh F, Gholizadeh P, Taghizadeh S, Ghanbarov K, Yousefi M and Kafil HS. Gut microbiota and colorectal cancer risk factors. Curr Pharm Biotechnol 2023; 24: 1018-1034.

[7] Tang X, Wang P, Huang S, Peng J, Zhang W, Shi X, Shi L, Zhong X, Lyu M, Zhou X and Linghu E. Trend of gastrointestinal and liver diseases in China: results of the global burden of disease study, 2019. Chin Med J (Engl) 2024; 137: 2358-2368.

[8] Li J, Yao H, Lu Y, Zhang S and Zhang Z; Society of Digestive Endoscopy of the Chinese Medical Association, Colorectal Surgery Group of the Chinese Medical Association, Chinese Association of Gastroenterologist & Hepatologist, National Clinical Research Center for Digestive Diseases, Chinese Medical Journal Clinical Practie Guideline Collaborative. Chinese national clinical practice guidelines on prevention, diagnosis and treatment of early colorectal cancer. Chin Med J (Engl) 2024; 137: 2017-2039.

[9] Tourelle KM, Boutin S, Weigand MA and Schmitt FCF. The association of gut microbiota and complications in gastrointestinal-cancer therapies. Biomedicines 2021; 9: 1305.
[10] Jia B, Han X, Kim KH and Jeon CO. Discovery and mining of enzymes from the human gut microbiome. Trends Biotechnol 2022; 40: 240-254.
[11] Cheng Y, Ling Z and Li L. The intestinal microbiota and colorectal cancer. Front Immunol 2020; 11: 615056.
[12] Zhao Y, Wang C and Goel A. Role of gut microbiota in epigenetic regulation of colorectal cancer. Biochim Biophys Acta Rev Cancer 2021; 1875: 188490.
[13] Jovanovic N, Zach V, Crocini C, Bahr LS, Forslund-Startceva SK and Franz K. A gender perspective on diet, microbiome, and sex hormone interplay in cardiovascular disease. Acta Physiol (Oxf) 2024; 240: e14228.
[14] Kossenas K and Constantinou C. Epidemiology, molecular mechanisms, and clinical trials: an update on research on the association between red meat consumption and colorectal cancer. Curr Nutr Rep 2021; 10: 435-467.
[15] Abdillah A and Ranque S. Chronic diseases associated with malassezia yeast. J Fungi (Basel) 2021; 7: 855.
[16] Liu Y, Lau HC, Cheng WY and Yu J. Gut microbiome in colorectal cancer: clinical diagnosis and treatment. Genomics Proteomics Bioinformatics 2023; 21: 84-96.
[17] Zheng Z, Hou X, Bian Z, Jia W and Zhao L. Gut microbiota and colorectal cancer metastasis. Cancer Lett 2023; 555: 216039.
[18] Fusco W, Bricca L, Kaitsas F, Tartaglia MF, Venturini I, Rugge M, Gasbarrini A, Cammarota G and Ianiro G. Gut microbiota in colorectal cancer: from pathogenesis to clinic. Best Pract Res Clin Gastroenterol 2024; 72: 101941.
[19] Kim YM, Choi JO, Cho YJ, Hong BK, Shon HJ, Kim BJ, Park JH, Kim WU and Kim D. Mycobacterium potentiates protection from colorectal cancer by gut microbial alterations. Immunology 2023; 168: 493-510.
[20] Reuvers JRD, Budding AE, van Egmond M, Stockmann HBAC, Twisk JWR, Kazemier G, Abis GSA and Oosterling SJ; SELECT trial group. Gut proteobacteria levels and colorectal surgical infections: SELECT trial. Br J Surg 2023; 110: 129-132.
[21] Kong C, Liang L, Liu G, Du L, Yang Y, Liu J, Shi D, Li X and Ma Y. Integrated metagenomic and metabolomic analysis reveals distinct gut-microbiome-derived phenotypes in early-onset colorectal cancer. Gut 2023; 72: 1129-1142.
[22] Shams K, Larypoor M and Salimian J. The immunomodulatory effects of Candida albicans isolated from the normal gastrointestinal microbiome of the elderly on colorectal cancer. Med Oncol 2021; 38: 140.
[23] Wang F, He MM, Yao YC, Zhao X, Wang ZQ, Jin Y, Luo HY, Li JB, Wang FH, Qiu MZ, Lv ZD, Wang DS, Li YH, Zhang DS and Xu RH. Regorafenib plus toripalimab in patients with metastatic colorectal cancer: a phase Ib/II clinical trial and gut microbiome analysis. Cell Rep Med 2021; 2: 100383.
[24] Oh B, Boyle F, Pavlakis N, Clarke S, Guminski A, Eade T, Lamoury G, Carroll S, Morgia M, Kneebone A, Hruby G, Stevens M, Liu W, Corless B, Molloy M, Libermann T, Rosenthal D and Back M. Emerging evidence of the gut microbiome in chemotherapy: a clinical review. Front Oncol 2021; 11: 706331.
[25] Schoeler M, Chakaroun R, Brolin H, Larsson I, Perkins R, Marschall HU, Caesar R and Backhed F. Moderate variations in the human diet impact the gut microbiota in humanized mice. Acta Physiol (Oxf) 2024; 240: e14100.
[26] Pidikova P, Reis R and Herichova I. miRNA clusters with down-regulated expression in human colorectal cancer and their regulation. Int J Mol Sci 2020; 21: 4633.
[27] Pedrosa LF and Fabi JP. Dietary fiber as a wide pillar of colorectal cancer prevention and adjuvant therapy. Crit Rev Food Sci Nutr 2024; 64: 6177-6197.
[28] Gilbert B, Kaiko G, Smith S and Wark P. A systematic review of the colorectal microbiome in adult cystic fibrosis patients. Colorectal Dis 2023; 25: 843-852.
[29] Wang X, Sun X, Chu J, Sun W, Yan S and Wang Y. Gut microbiota and microbiota-derived metabolites in colorectal cancer: enemy or friend. World J Microbiol Biotechnol 2023; 39: 291.
[30] Jia R, Shao S, Zhang P, Yuan Y, Rong W, An Z, Lv S, Feng Y, Liu N, Feng Q, Wang Y and Li Q. PRM1201 effectively inhibits colorectal cancer metastasis via shaping gut microbiota and short- chain fatty acids. Phytomedicine 2024; 132: 155795.
[31] Xiong M, Liu Z, Wang B, Sokolich T, Graham N, Chen M, Wang WL and Boldin MP. The epithelial C15ORF48/miR-147-NDUFA4 axis is an essential regulator of gut inflammation, energy metabolism, and the microbiome. Proc Natl Acad Sci U S A 2024; 121: e2315944121.
[32] Qiao S, Wu D, Wang M, Qian S, Zhu Y, Shi J, Wei Y and Lai H. Oral microbial profile variation during canine ligature-induced peri-implantitis development. BMC Microbiol 2020; 20: 293.
[33] Miyoshi T, Oge S, Nakata S, Ueno Y, Ukita H, Kousaka R, Miura Y, Yoshinari N and Yoshida A. Gemella haemolysans inhibits the growth of the periodontal pathogen Porphyromonas gingivalis. Sci Rep 2021; 11: 11742.

[34] Lopes EM, Passini MRZ, Kishi LT, Chen T, Paster BJ and Gomes BPFA. Interrelationship between the microbial communities of the root canals and periodontal pockets in combined endodontic-periodontal diseases. Microorganisms 2021; 9: 1925.
[35] Sugino KY, Ma T, Paneth N and Comstock SS. Effect of environmental exposures on the gut microbiota from early infancy to two years of age. Microorganisms 2021; 9: 2140.
[36] Hua X, Zhu J, Yang T, Guo M, Li Q, Chen J and Li T. The Gut microbiota and associated metabolites are altered in sleep disorder of children with autism spectrum disorders. Front Psychiatry 2020; 11: 855.
[37] Shuwen H, Xi Y, Yuefen P, Jiamin X, Quan Q, Haihong L, Yizhen J and Wei W. Effects of postoperative adjuvant chemotherapy and palliative chemotherapy on the gut microbiome in colorectal cancer. Microb Pathog 2020; 149: 104343.
[38] Xu J, Yang M, Wang D, Zhang S, Yan S, Zhu Y and Chen W. Alteration of the abundance of Parvimonas micra in the gut along the adenoma-carcinoma sequence. Oncol Lett 2020; 20: 106.
[39] Ibeanu GC, Rowaiye AB, Okoli JC and Eze DU. Microbiome differences in colorectal cancer patients and healthy individuals: implications for vaccine antigen discovery. Immunotargets Ther 2024; 13: 749-774.
[40] Wu Z, Sun Y, Huang W, Jin Z, You F, Li X and Xiao C. Direct and indirect effects of estrogens, androgens and intestinal microbiota on colorectal cancer. Front Cell Infect Microbiol 2024; 14: 1458033.

Supplementary Table 1. Primer list

hsa-mir-21	5'-CAACACCAGUCGAUGGGCUGU-3'
RTP	5'-GTCGTATCCAGTGCAGGGTCCGAGGTATTCGCACTGGATACGACACAGCC-3'
PCRM	5'-CAACACCAGTCGATGGGCTGTGTCGTATCCAGTGCGAATACCTCGGACCCTGCACTGGATACGAC-3'
F-PCR	5'-GCGCAACACCAGTCGATG-3'
R-PCR	5'-AGTGCAGGGTCCGAGGTATT-3'
hsa-mir-31	5'-UGCUAUGCCAACAUAUUGCCAU-3'
RTP	5'-GTCGTATCCAGTGCAGGGTCCGAGGTATTCGCACTGGATACGACATGGCA-3'
PCRM	5'-TGCTATGCCAACATATTGCCATGTCGTATCCAGTGCGAATACCTCGGACCCTGCACTGGATACGAC-3'
F-PCR	5'-CGCGTGCTATGCCAACATAT-3'
R-PCR	5'-AGTGCAGGGTCCGAGGTATT-3'
hsa-mir-135a	5'-UAUAGGGAUUGGAGCCGUGGCG-3'
RTP	5'-GTCGTATCCAGTGCAGGGTCCGAGGTATTCGCACTGGATACGACCGCCAC-3'
PCRM	5'-TATAGGGATTGGAGCCGTGGCGGTCGTATCCAGTGCGAATACCTCGGACCCTGCACTGGATACGAC-3'
F-PCR	5'-CGCGTATAGGGATTGGAGCC-3'
R-PCR	5'-AGTGCAGGGTCCGAGGTATT-3'
hsa-mir-106a	5'-CUGCAAUGUAAGCACUUCUUAC-3'
RTP	5'-GTCGTATCCAGTGCAGGGTCCGAGGTATTCGCACTGGATACGACGTAAGA-3'
PCRM	5'-CTGCAATGTAAGCACTTCTTACGTCGTATCCAGTGCGAATACCTCGGACCCTGCACTGGATACGAC-3'
F-PCR	5'-CGCGCTGCAATGTAAGCACT-3'
R-PCR	5'-AGTGCAGGGTCCGAGGTATT-3'
hsa-mir-135b	5'-AUGUAGGGCUAAAAGCCAUGGG-3'
RTP	5'-GTCGTATCCAGTGCAGGGTCCGAGGTATTCGCACTGGATACGACCCCATG-3'
PCRM	5'-ATGTAGGGCTAAAAGCCATGGGGTCGTATCCAGTGCGAATACCTCGGACCCTGCACTGGATACGAC-3'
F-PCR	5'-CGCGATGTAGGGCTAAAAGC-3'
R-PCR	5'-AGTGCAGGGTCCGAGGTATT-3'
hsa-mir-143	5'-UGAGAUGAAGCACUGUAGCUC-3'
RTP	5'-GTCGTATCCAGTGCAGGGTCCGAGGTATTCGCACTGGATACGACGAGCTA-3'
PCRM	5'-TGAGATGAAGCACTGTAGCTCGTCGTATCCAGTGCGAATACCTCGGACCCTGCACTGGATACGAC-3'
F-PCR	5'-CGCGTGAGATGAAGCACTG-3'
R-PCR	5'-AGTGCAGGGTCCGAGGTATT-3'
hsa-mir-145	5'-GGAUUCCUGGAAAUACUGUUCU-3'
RTP	5'-GTCGTATCCAGTGCAGGGTCCGAGGTATTCGCACTGGATACGACAGAACA-3'
PCRM	5'-GGATTCCTGGAAATACTGTTCTGTCGTATCCAGTGCGAATACCTCGGACCCTGCACTGGATACGAC-3'
F-PCR	5'-CGCGGGATTCCTGGAAATAC-3'
R-PCR	5'-AGTGCAGGGTCCGAGGTATT-3'